Figure S1. Curie plots of the pyrrole protons in some [Fe(TMP)L]ClO_4 where axial ligands(L's) are less hindered imidazoles such as HIm, 1-MeIm, and 5-MeIm.

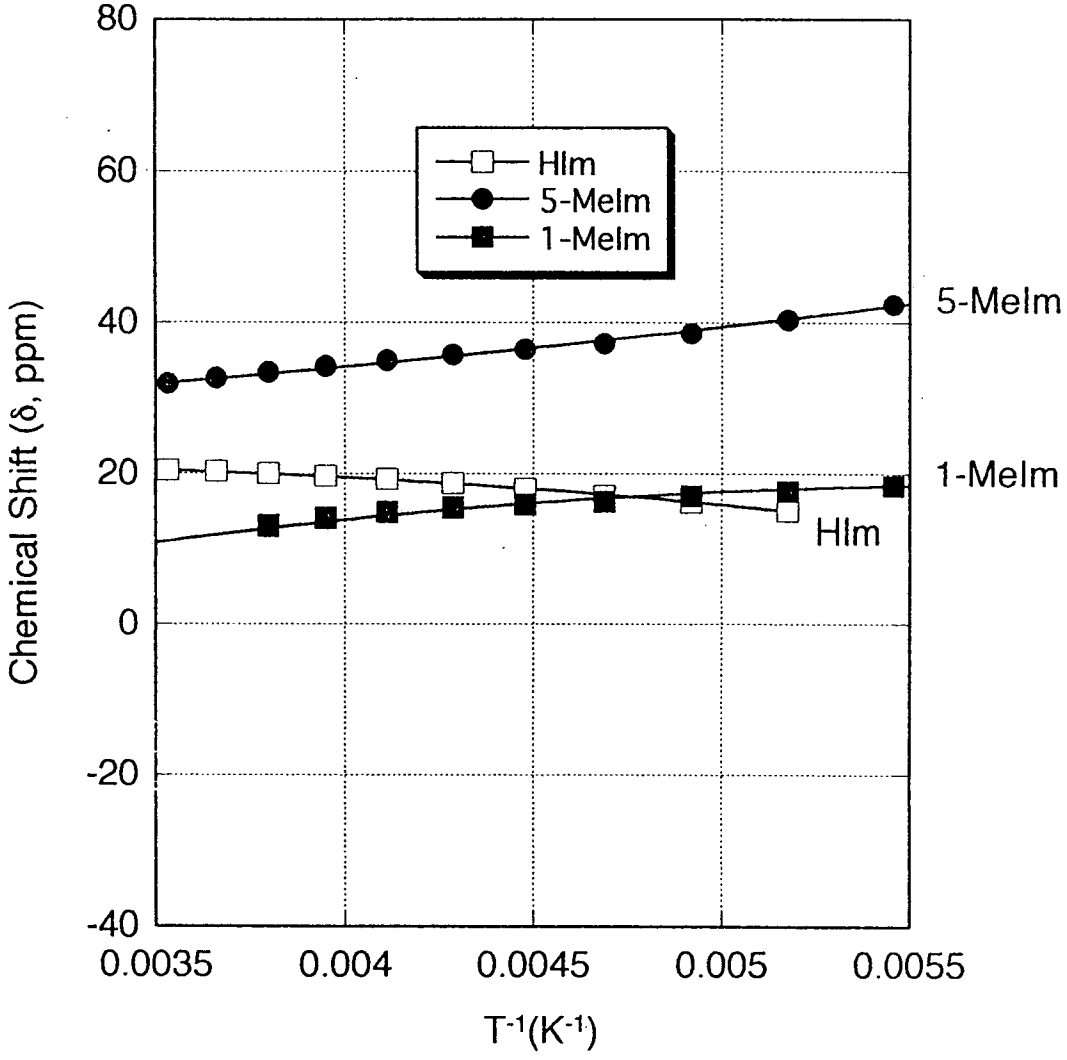

Figure S2. Curie plots of the pyrrole protons in some [Fe(TMP)L]ClO_4 where axial ligands(L's) are 1-Me-2-RIm(R = Me, Et, or ^{i}Pr).

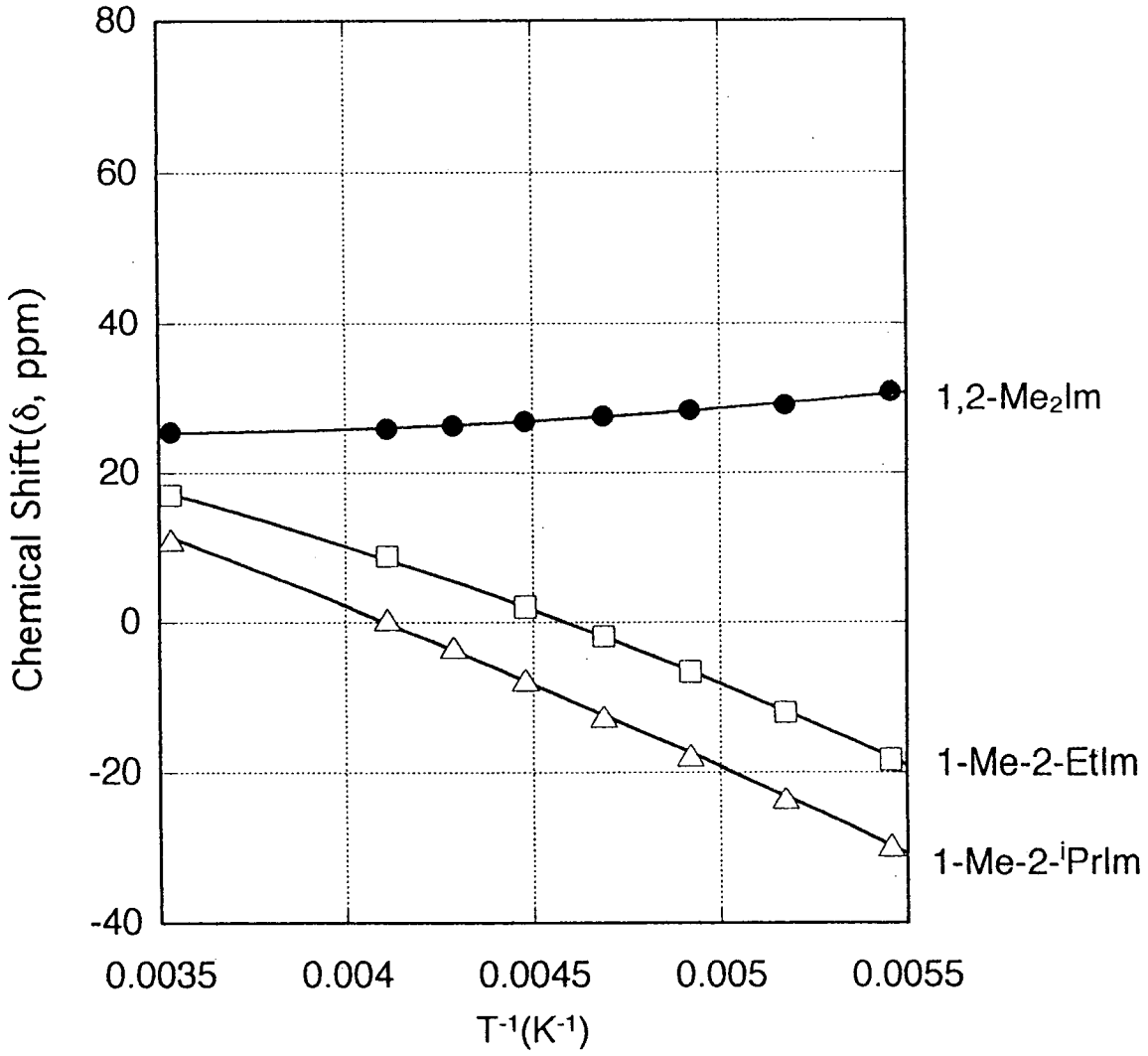

Figure S3. Curie plots of the pyrrole protons in some $[Fe(TMP)L]ClO_4$ where axial ligands(L's) are substituted benzimidazoles.

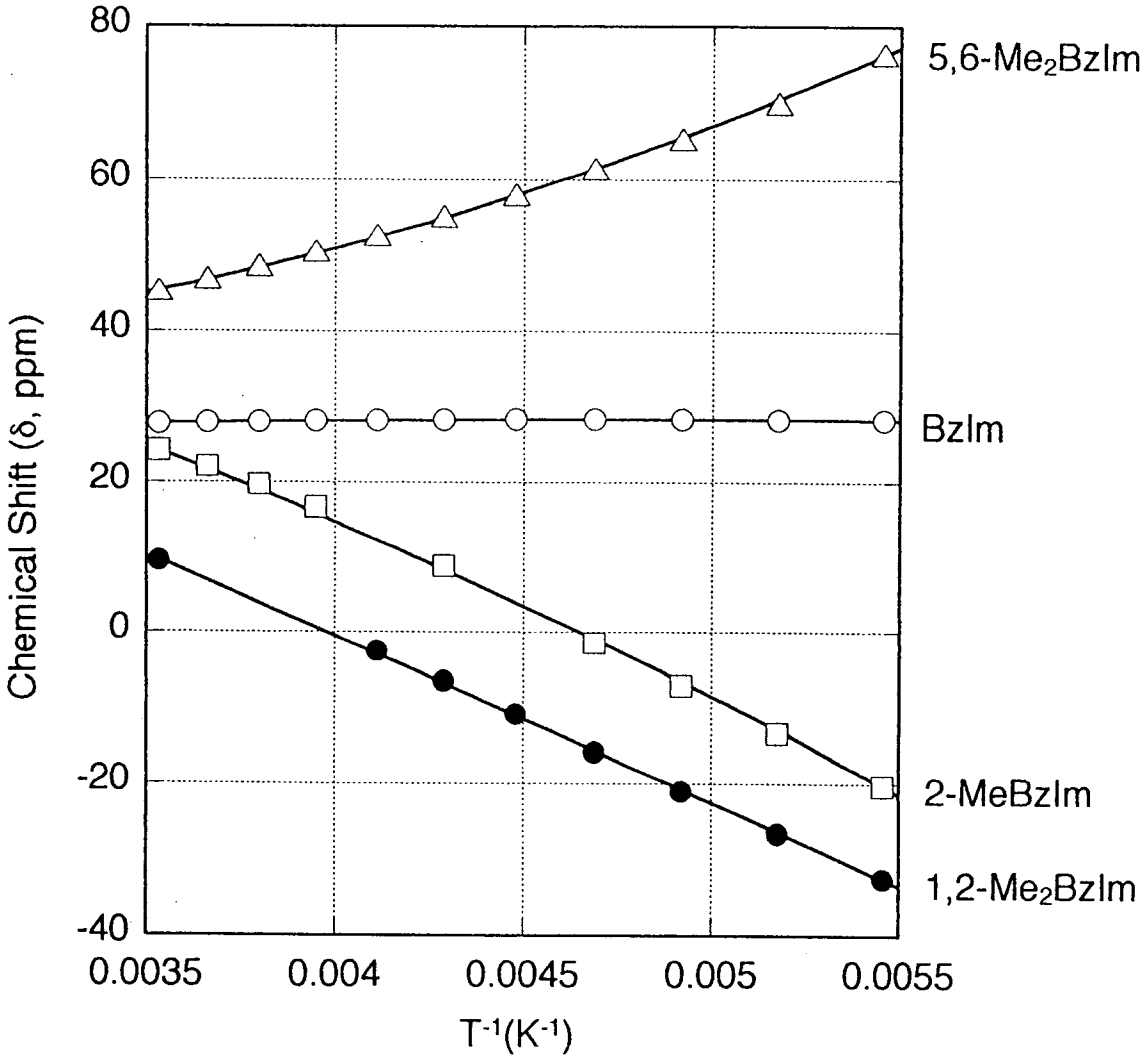

Figure S4. Curie plots of the *meso* carbons in some $[Fe(TMP)L]ClO_4$.

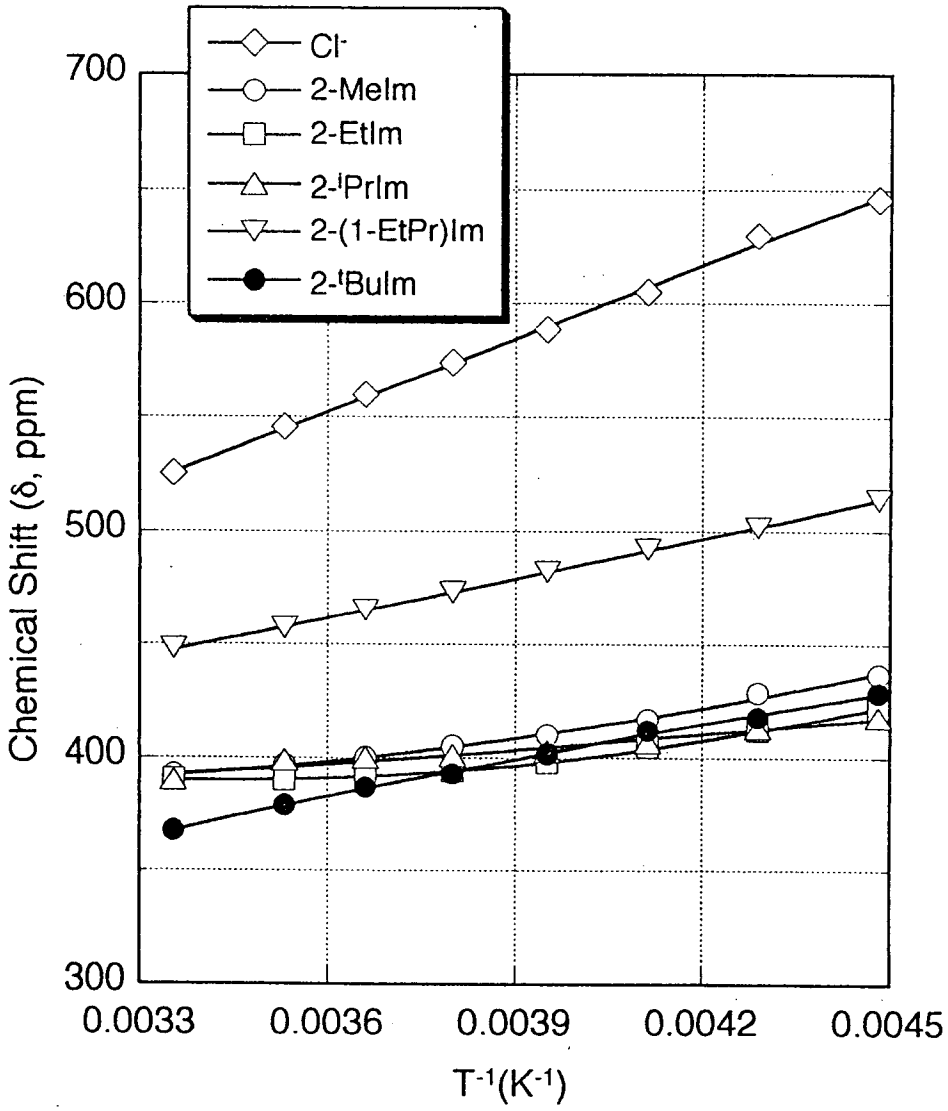

Figure S5. Curie plots of the α-pyrrole carbons in some $[Fe(TMP)L]ClO_4$.

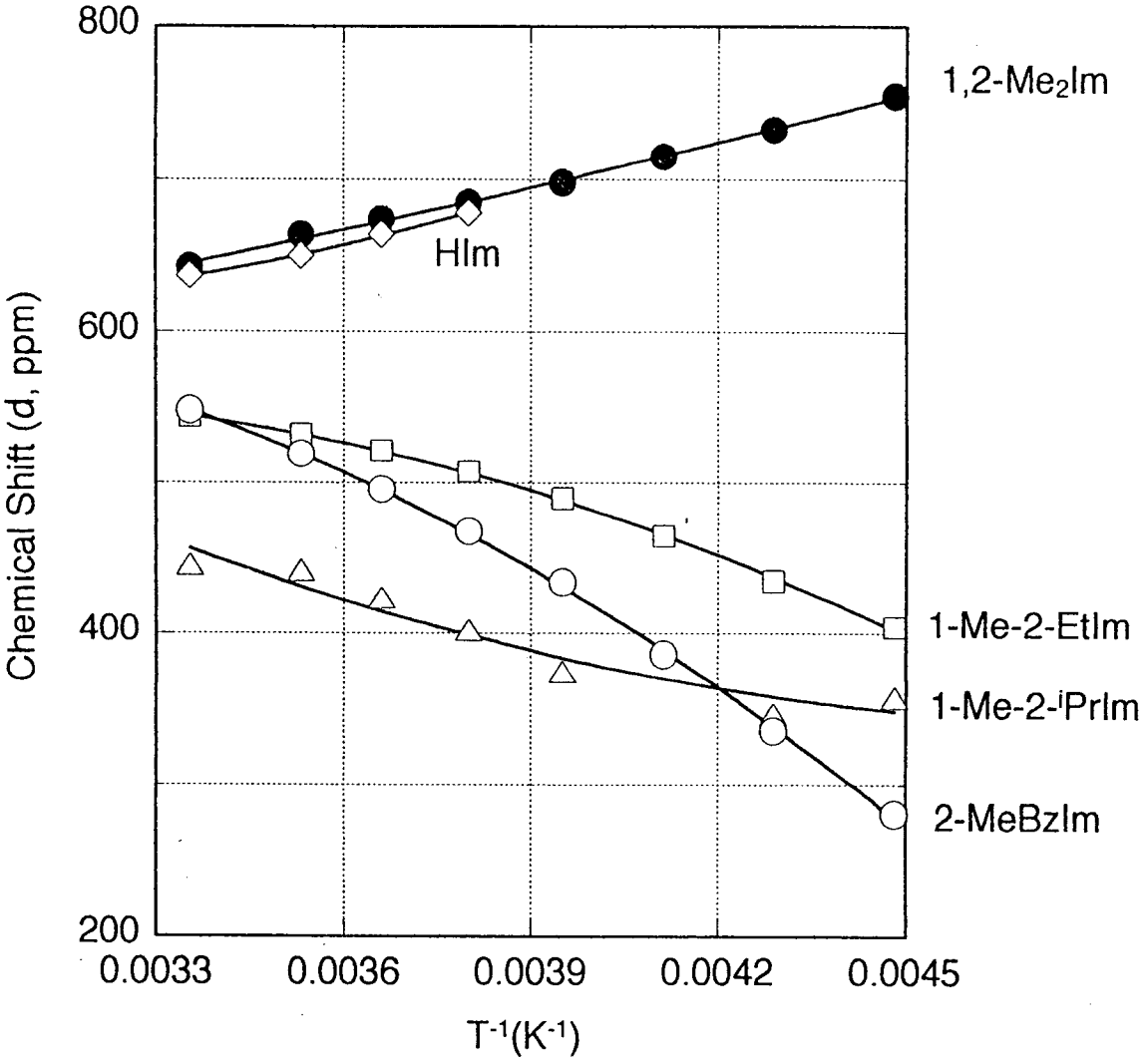

Figure S6. Curie plots of the β-pyrrole carbons in some $[Fe(TMP)L]ClO_4$.

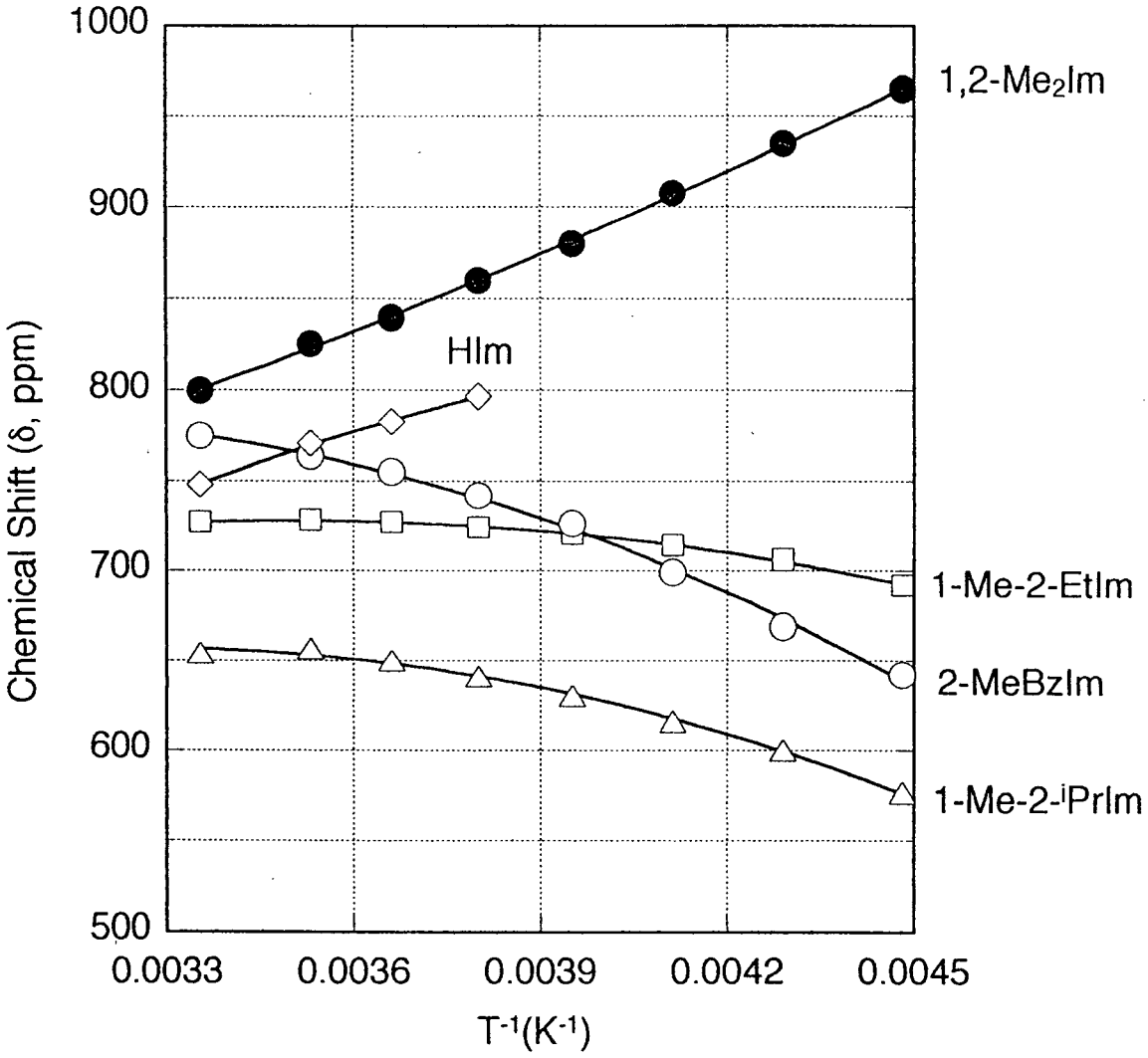

Figure S7. Curie plots of the *meso* carbons in some $[Fe(TMP)L]ClO_4$.

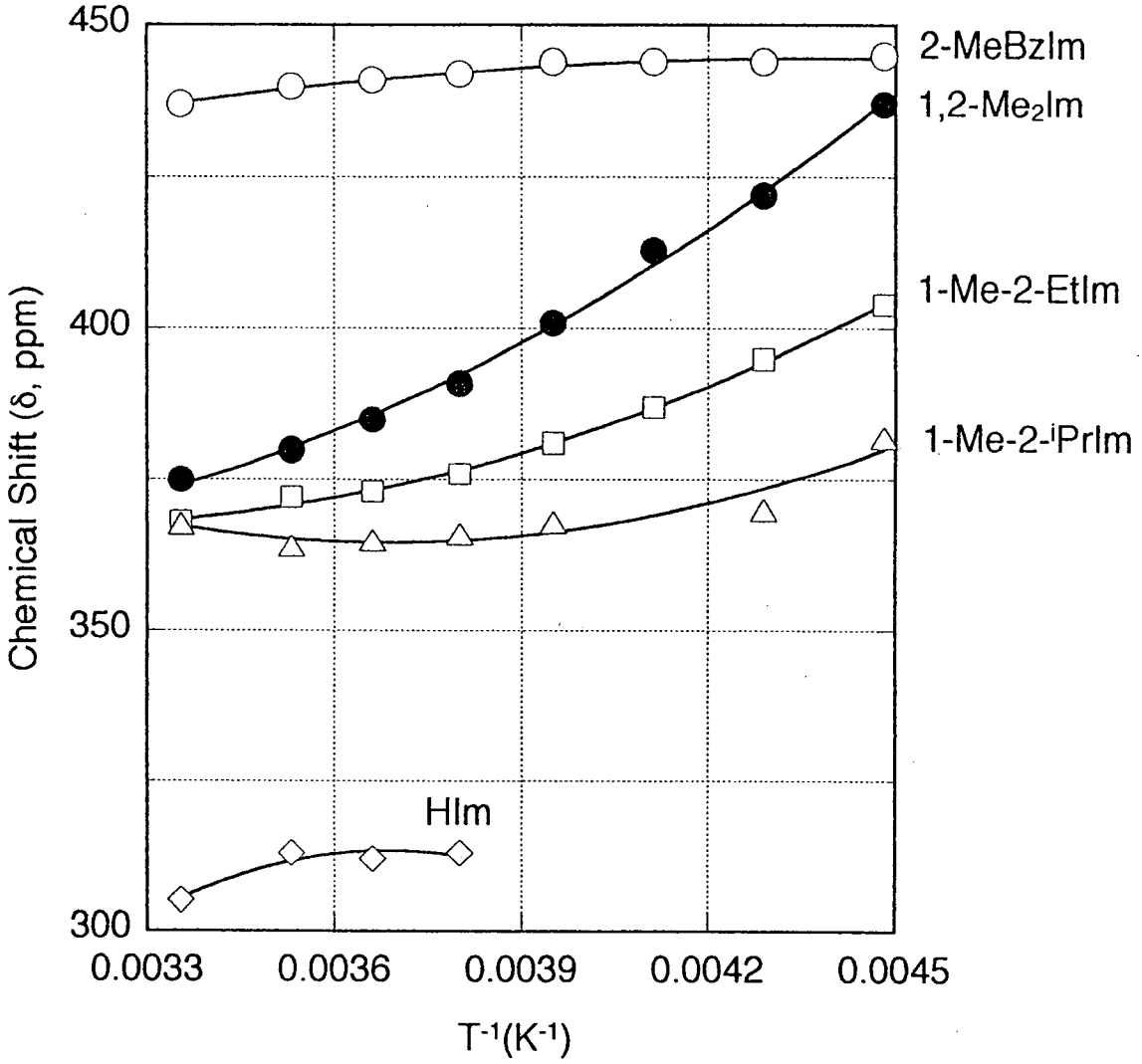

Table S1. ^{1}H NMR Chemical Shifts(δ, ppm) of Some Protons of Coordinated Imidazoles in [Fe(TMP)L]ClO_4 Determined at 25 °C in CD_2Cl_2 Solution.

Axial Ligands	1-H(CH_3)	4-H	5-H(CH_3)
HIm	48.0	99.6	84.3
5-MeIm	a)	100.1	(21.5)
2-MeIm	54.0	110.7	67.0
2-EtIm	77.4	115.1	65.0
2-^{i}PrIm	61.8	116.9	77.0
2-(1-EtPr)Im	63.8	120.2	78.2
2-^{t}BuIm	b)	b)	b)
1,2-Me_2Im	(21.5)	77.8	70.0
1-Me-2-EtIm	(19.9)	77.7	66.5
1-Me-2-^{i}PrIm	(19.1)	78.3	65.7

a) Signal is too broad to detect. b) Signals are broad due to the ligand exchange.